Progress in Oceanography 239 (2025) 103594

Contents lists available at ScienceDirect

Progress in Oceanography

journal homepage: www.elsevier.com/locate/pocean

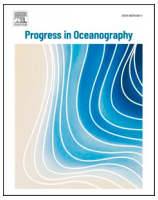

Trenches apart, yet worm to worm: inter- and intra-trench comparisons reveal divergent and convergent dynamics in hadal nematode biodiversity☆

Yick Hang Kwan [a,*], Sofie Derycke [d,e], Blandine Trouche [a], Frank Wenzhöfer [a,f,g], Mathias Middelboe [a,h], Angelika Brandt [i,j], Mauricio Shimabukuro [a,b], Ronnie N. Glud [a,k,l], Daniela Zeppilli [c]

[a] HADAL & Nordcee, Department of Biology, University of Southern Denmark, Campusvej 55, 5230 Odense, Denmark
[b] Instituto de Oceanografia, Universidade Federal do Rio Grande, Rio Grande, Brazil
[c] Univ. Brest, Ifremer, BEEP, F-29280 Plouzané, France
[d] Animal Science Unit, Flanders Research Institute for Agriculture, Fisheries and Food, ILVO, Aquatic Environment and Quality, Ostend, Belgium
[e] Marine Biology Section, Department of Biology, Ghent University, Ghent, Belgium
[f] HGF-MPG Joint Research Group for Deep-Sea Ecology and Technology, Alfred-Wegener-Institute, Helmholtz Centre for Polar and Marine Research, Am Handelshafen 12, Bremerhaven, Germany
[g] HGF-MPG Joint Research Group for Deep-Sea Ecology and Technology, Max Planck Institute for Marine Microbiology, Celsiusstraße 1, 28359 Bremen, Germany
[h] Marine Biological Section, Department of Biology, University of Copenhagen, Strandpromenaden 5, 3000 Helsingør, Denmark
[i] Department of Marine Zoology, Senckenberg Research Institute and Natural History Museum, Frankfurt, Germany
[j] Faculty of Biological Sciences, Institute of Ecology, Diversity and Evolution, Goethe University, Frankfurt, Germany
[k] Danish Institute for Advanced Study (DIAS), University of Southern Denmark, Campusvej 55, 5230 Odense, Denmark
[l] Department of Ocean and Environmental Sciences, Tokyo University of Marine Science and Technology, 4-5-7 Konan, Minato-ku, 108-8477 Tokyo, Japan

ARTICLE INFO

Keywords:
Hadal
Aleutian Trench
South Sandwich Trench
Hadal nematode
eDNA
Metaphylogeography

ABSTRACT

The hadal zone, the deepest part of the global ocean, encompasses several extreme ecosystems with elevated biological activity, contrasting the general trend of declining biomass and biodiversity with increasing water depth. These bathymetrically isolated habitats act as depocenters and are characterized by high hydrostatic pressure and unique environmental conditions that provide an opportunity to fundamentally explore biogeographic patterns and the genetic diversity of deep-sea meiofauna, which remain poorly understood. In this study, we compared nematode communities in two geographically distant trench systems, the Aleutian Trench (North Pacific) and the South Sandwich Trench (South Atlantic), separated by 17 000 km. Environmental DNA (eDNA) sequencing targeting the ribosomal 18S region was combined with a metaphylogeography approach. Comparative analyses were performed for intra- and inter-trench, biodiversity and genetic differentiation across environmentally characterised trench-specific habitats. Our findings reveal evidence for the meiofauna paradox in hadal settings, demonstrating distinct nematode communities that appear to be shaped by availability and quality of food. Furthermore, environmental filtering appeared to contribute to assembly of habitat specific communities according to localised environmental condition. Finally, we observed shared haplotypes among some dominating nematode genera, suggesting potential connectivity between habitats associated within or even across hadal trenches might exist. Overall, this study provides valuable insights on how environmental factors drive nematode biodiversity and genetic diversity in the hadal realm. Environmental heterogeneity plays a pivotal role in shaping nematode communities, influencing their population structure and connectivity by creating spatially variable habitats that drive diversification, local adaptation, and gene flow patterns.

1. Introduction

Abundance and biomass of fauna generally decline with increasing water depth due to reduced food availability (Rex et al., 2006). The limitation in nutritious energy may reduce the potential of diversification and endemism within the bathyal and abyssal realm (Rex et al.,

☆ This article is part of a special issue entitled: 'AleutBio' published in Progress in Oceanography.

* Corresponding author.
E-mail address: yick@sdu.dk (Y.H. Kwan).

https://doi.org/10.1016/j.pocean.2025.103594

Available online 15 October 2025

2006; Smith et al., 2008). However, in the hadal realm, these patterns seem to be inverted (Jamieson, 2015; Zeppilli et al., 2018). Trenches, accounting for 94 % of the area of hadal habitats (Weston and Jamieson, 2022), stretch thousands of kilometres along tectonic subduction zones (Jamieson et al., 2010), and include depths between 6 to 11 km, accounting for 45 % of the oceanic depth range (Liu et al., 2018). Trenches function as deep-sea depocenters, where downslope focusing of material—amplified by intensified seismic activity—enhances the accumulation of organic matter along the trench axes (Bao et al., 2018) where it sustains elevated biological activity (Glud et al., 2021; Glud et al., 2013). The trenches represent bathymetrically isolated environments and host many endemic species or genera adapted to high hydrostatic pressure (Blankenship-Williams and Levin, 2009; Jamieson, 2015; Jamieson and Stewart, 2021). However, trench environments are heterogeneous and highly variable, shaped by factors such as regional bathymetry, proximity to land, and varying physical and chemical conditions—all of which play a crucial role in structuring the biological communities within individual trenches. (Jamieson et al., 2010; Kitahashi et al., 2013; Liu et al., 2018). The high degree of endemism in hadal trenches is likely associated with the adaptation to extreme hydrostatic pressure, that confines vertical movements of well adapted species, restricts communities' distribution area (Lan et al., 2017), and limits connectivity to the ambient ocean and other trench systems (Fujii et al., 2013). Thus genetical, morphological, behavioural or physiological modifications during hadal colonization reduce the potential for dispersal and genetic exchange outside a trench area (Chan et al., 2020; Gerringer et al., 2018). However, current concepts on hadal endemism are primarily based on epibenthic macro- and megafaunas as well as mobile species inhabiting the benthic boundary layer (Chan et al., 2020; Gerringer et al., 2018), while biogeographic patterns of meiofaunal or microbial communities are rarely considered (Leduc and Rowden, 2018; Zeppilli et al., 2018).

Meiofauna are microscopic metazoans passing through a 1 mm mesh but retained by a 32 μm mesh. They are ubiquitous and recognized as an important component of marine benthic ecosystems, yet described as sedentary (Giere, 2009; Giere and Schratzberger, 2023; Rosli et al., 2018; Schratzberger and Ingels, 2018; Zeppilli et al., 2018). This phenomenon – a fact that is known as the "meiofauna-paradox"- is observed in almost all meiofaunal taxa, including but not limited to harpacticoid copepods, gastrotrichs, kinorhynchs and nematodes (Cerca et al., 2018; Giere, 2009; Vanreusel et al., 2023). Nematodes represent the most abundant and diverse meiofauna group, and clearly dominate deep-sea meiofaunal communities throughout the global oceans (Miljutin et al., 2010; Zeppilli et al., 2018). As noted, the high standing stock of hadal nematodes is likely sustained by elevated or nutritious food supply as expressed by tight correlation between microbial metabolic activity and nematode biomass – both at local, inter and intra trench spatial scale (Glud and Schauberger, 2024; Shimabukuro et al., 2022). Generally, studies on nematode communities in the deep sea tend to focus on the composition, density or biomass, and to a lesser extent on biogeographic patterns or potential genetic endemism within or between trenches (Schmidt et al., 2018; Zeppilli et al., 2018). Investigations on coastal margins and continental slopes concluded that some nematode genera or species can have wide geographic distributions, as seen by *Litoditis marina* (Bastian, 1865), and express little diversification even between distant populations (Derycke et al., 2013). However, is the "*meiofauna paradox*" also prevalent in nematodes from the extreme and bathymetrically isolated environments of the hadal realm?

To unveil the potential of nematode dispersal in the deepest part of the global ocean, we compared nematode assemblages in two distant trenches separated by 17 000 km: the Aleutian Trench (AT) in the North Pacific Ocean, and the South Sandwich Trench (SST) in the South Atlantic Ocean. Intra-and-inter habitat comparisons in the two trench areas were conducted according to trench related habitats based on location, water depth, total organic carbon content and microbial abundance. The investigations were based on environmental DNA (eDNA) extracted from recovered sediments and the Amplicon Sequence Variants (ASVs) of metazoans/nematodes as expressed by the ribosomal 18S region exposed to a metaphylogeography bioinformatic pipeline (Turon et al., 2020).

The main goal of our study was to utilise genetic data of nematode assemblages to investigate the *meiofauna-paradox* in deep-sea settings: *Is everywhere different, but something is everywhere?* The specific objectives were to 1) compare the intra-and-inter trench nematode communities and the respective diversity of the two targeted trenches, 2) explore potential endemism of nematode communities in each of the two trenches and, 3) examine the genetic differentiation within widespread and abundant nematode genera within and across the trench systems. The insight gained is used to assess and discuss genetic diversity and whether geographical isolation of trenches affect nematode population structure and connectivity.

2. Materials and methods

2.1. Sediment collection

Sediment cores from the Aleutian and the South Sandwich Trenches were collected by multiple corers (MUC) during two separate seagoing expeditions with RV *Sonne*, (Cruise No. SO293, 2022) (Brandt, 2023; Brandt et al., 2025) and RV *Polarstern*, (Cruise No. PS133/1, 2022) (Klaas et al., 2023), respectively. Upon recovery, sediment cores (diameter: 95 mm) were brought to a thermoregulated laboratory kept at 4 °C, and surface sediment slices (0–1 cm) were stored in plastic bags at −80 °C until analysis.

In total 14 stations were visited in the Aleutian Trench area (Fig. 1b). The three stations at the Northern slope (NS) ranged from 4.3 to 4.6 km of depth, had relatively high Total Organic Carbon (TOC) content and relatively high microbial abundance (Sindlev et al., 2025). The three stations at the Southern slope (SS) ranged from 4.8 to 5.3 km of depth, were deprived in TOC and had very low microbial abundance (Sindlev et al., 2025). The seven stations inside the trench ranged from 6.3 to 7.2 km of depth and most sites were covered by a 2 to 25 cm layer of fine-grained glacial erosion material – that appeared like a "*fluid mud layer*" (FML) (Sindlev et al., 2025) (Table 1). One reference station at 3.6 km of depth was located in the Bering Seas (BS), separated from the trench system by the Aleutian archipelago and a distance of 500 km. In total four stations were visited in the South Sandwich Trench area (Fig. 1c). These included i) one 5 km deep station at the trench slope, that had moderate TOC content and high microbial abundances, ii) one station within the actual trench, at 8 km water depth, that had relatively high TOC content but relatively low microbial abundances, iii) finally, two distinct reference stations located at 3.5 km and 3.8 km of depth, 1500 km to the northeast and northwest of the trench system, respectively (Klaas et al., 2023). The northeast reference station was characterised by low TOC content and relatively low microbial abundances, while the northwest reference station had high TOC content and relatively higher microbial abundances (Table 1). The 18 stations were grouped into nine sampling habitats depending on their location, depths, TOC content and microbial abundances for further biogeographic investigations: Aleutian Trench reference (AT-Ref), Aleutian Trench northern slope (AT-NS), Aleutian Trench southern slope (AT-SS), Aleutian Trench axis with and without FLM respectively (AT+FML, −FML), South Sandwich Trench northeast reference (SST-Ref1), South Sandwich Trench northwest reference (SST-Ref2), South Sandwich Trench eastern slope (SST-S) and South Sandwich Trench axis (SST-A) (Table 1). Bathymetry data were extracted from the GEBCO online database and maps were constructed using the software packages ggmap and QGIS v3.42.3. The trench locations and, details for each sampling stations are shown in Fig. 1 and Table 1.

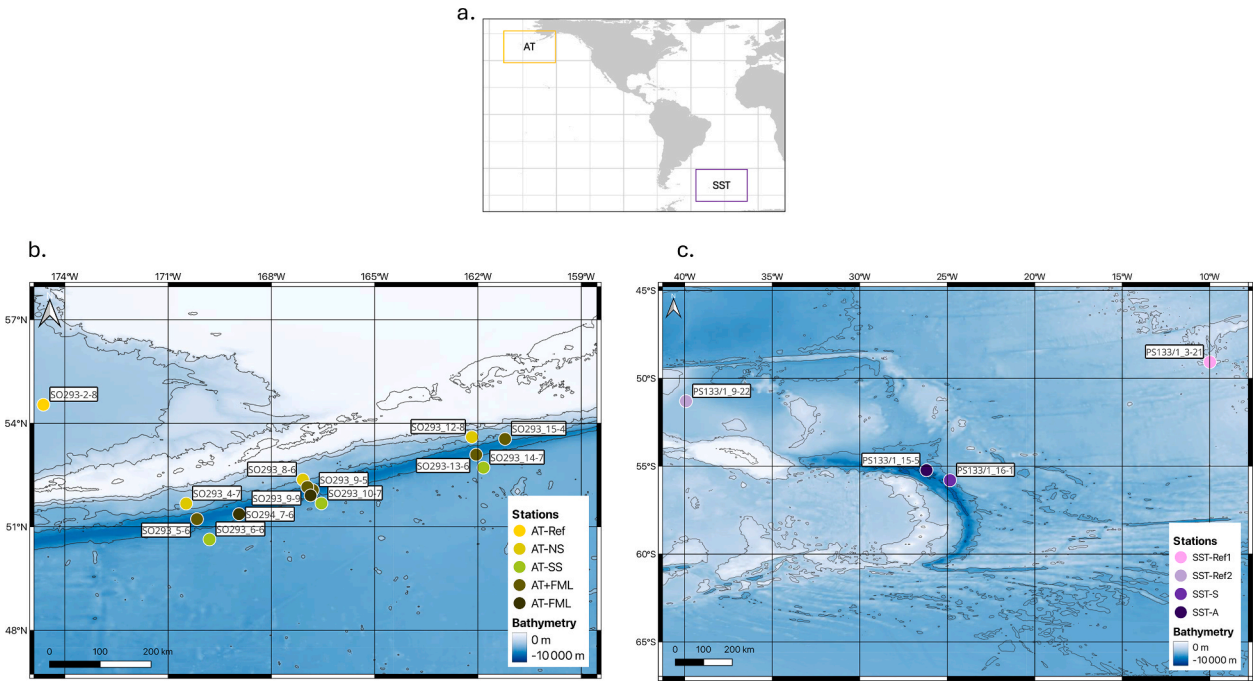

Fig. 1. Map of the two-sampling trench, and the respective sampling station. **1a.** Location of the trench systems on world map. Yellow grid indicates the Aleutian Trench sampling area and purple grid indicates the South Sandwich Trench sampling area. **1b.** The 14 stations in the Aleutian Trench area. **1c.** The four stations in the South Sandwich Trench area.

Table 1
Details of 18 sampling stations, the trench system and corresponding sampling habitats in this study.

Stations	Water Depth (m)	Latitude	Longitude	TOC (wt %)#	Cell Counts (1 x 10^6)#	Remarks
Aleutian Trench (AT) – habitats						
Aleutian Trench reference (AT-Ref)						
SO293_2-8	3652	54.53	−174.62	0.80	3.41	Bering Seas (BS)
Aleutian Trench northern slope (AT-NS)						
SO293_4-7	4642	51.67	−170.48	0.69	10.80	Northern Slope (NS)
SO293_8-6	4610	52.37	−167.08	0.64	1.73	Northern Slope
SO293_12-8	4304	51.67	−170.47	1.08	19.80	Northern Slope
Aleutian Trench southern slope (AT-SS)						
SO293_6-6	5316	50.63	−169.80	0.44	14.00	Southern Slope (SS)
SO293_10-7	5098	51.68	−166.54	0.26	6.39	Southern Slope
SO293_14-7	4871	52.71	−161.84	0.42	13.00	Southern Slope
Aleutian Trench axis with fluid mud layer (AT+FML)						
SO293_5-6	7237	51.22	−170.16	1.04	4.21	+ FML
SO293_9-5	7137	52.07	−166.80	0.90	3.46	+ FML
SO293_9-9	6475	52.15	−166.95	0.74	2.76	+ FML
SO293_13-6	6342	53.09	−162.05	0.78	1.72	+ FML
SO293_15-4	6265	53.54	−161.21	1.02	15.40	+ FML
Aleutian Trench axis without fluid mud layer (AT-FML)						
SO293_7-6	7212	51.37	−168.94	0.78	16.10	− FML
SO293_9-14	6500	51.91	−166.86	0.51	14.60	− FML
South Sandwich Trench (SST) – habitats						
South Sandwich Trench northeast reference (SST-Ref1)						
PS133/1_3-21	3421	−49.07	−9.99	0.24	16.50	Northeast reference
South Sandwich Trench northwest reference (SST-Ref2)						
PS133/1_9-22	3795	−51.30	−39.93	0.69	202.00	Northwest reference
South Sandwich Trench eastern slope (SST-S)						
PS133/1_16-1	5002	−55.23	−26.19	0.40	257.00	Eastern slope
South Sandwich Trench axis (SST-A)						
PS133/1_15-5	8066	−55.80	−24.84	0.23	65.80	Trench axis

#Measurement data for 0–1 cm layer.

2.2. Environmental parameters collection

During both expeditions, numerous chemical, physical and biological benthic parameters were analysed according to Sindlev et al. (2025) and Schauberger et al. (2021). For the current study we selected parameters that we considered of relevance for the assembly of meiofauna and nematode communities. These included: Mean grain size, sand content, silt content, clay content, total organic carbon (TOC) content, total nitrogen (TN) content, and cell counts (Table S1). Pearson correlation was used to statistically test the significance of linear-

relationships among environmental factors, using the R packages FactoMineR and corrplot (Lê et al., 2008; Wei et al., 2017). Highly intercorrelated environmental factors were excluded during subsequent analysis as described in Trouche et al. (2021).

2.3. DNA extraction, PCR amplification and sequencing

In the laboratory, 10 g of sediments from each of the surface slices were processed for extraction of meiofaunal DNA (Gielings et al., 2021). Two parallel sediment cores from the same MUC-cast, were used as biological duplicates (total sediment samples, n = 38). We applied the DNAeasy PowerMax Soil Kit (QIAGEN, USA) for extraction according to the manufacturer protocol and the final elution volume was adjusted to 1 mL to ensure a concentrated DNA extracts for PCR. Negative extraction controls were performed with 10 mL sterile Mili-Q water instead of sediment samples. The DNA concentration of the extracts was measured with the ds-DNA Quantitation, HS kit (ThermoFisher, USA) on a Qubit 4 Fluorometer (ThermoFisher, USA) according to the manufactory protocol. The DNA extracts were then kept at −20 °C prior to PCR amplifications (n = 39, including extraction negative).

The metabarcoding library preparation was done using primer pair SSU_04F and SSU_22R which amplifies a 360 bp DNA target region of the ribosomal 18S V1-V2 (Ahmed et al., 2019; Blaxter et al., 1998; Schenk et al., 2020). PCR reactions of each duplicate sediment sample were run as technical triplicates. We used 12.5 μL KAPA Taq HotStart polymerase ReadyMix (Kapa Biosystems, USA) with nuclease proofreading, 0.5 μL (concentration: 10 pmol/μL) of the forward and reverse primer, 0.5 μL BSA (ThermoFisher, USA), 9 μL of PCR Water (ThermoFisher, USA) and 2 μL of template for the 25 uL PCR reaction mix. Negative control for PCR was performed by replacing the template with PCR Water. The initial PCR amplifications were performed at the following condition: 2 mins at 95 °C, 30 cycles: 30 s at 95 °C, 60 s at 68 °C and 30 s at 72 °C, then 3 mins at 72 °C for final extension. The purified PCR products were then used for a second-step PCR with MiSeq adapter together with the primer's sequences for 12 cycles. The PCR products were purified as described above. A 3rd PCR for Illumina indexing was performed according to the manufactory protocol. Same index was used for the PCR products originated from the same sediment eDNA. In all three runs the PCR products were purified by 0.8x AMPure XP beads (Beckman Coulter, USA) and the DNA concentration of the final product was measured and normalized to same concentration and sequenced on a desktop Illumina MiSeq sequencer (Illumina, USA), with the MiSeq reagent kit v3 (Illumina, USA) for the 2x300 bp paired-end run with a target to generate 50,000 reads per sample (n = 40, including PCR negative control).

2.4. Sequence data analysis

The successfully base-called and demultiplexed raw sequenced data (n = 29) were first processed with Cutadapt v1.12 (Martin, 2011) for adapter and primer sequence removal. The following bioinformatic analysis was performed in R studio with various R packages in default settings and visualised with the R package ggplot (Villanueva and Chen, 2019) unless settings were specified individually. The truncated sequences were then used for ASVs generation following the DADA2 pipeline (Callahan et al., 2016) including the pipeline for the denoising, quality filtering, paired-end reads merging and chimera removal. The number of reads and ASVs per samples for each step were recorded (Supplementary Table II). Taxonomical assignment for these ASVs was done using the 18S_Silva_Nematoda_marine_18991 reference database containing manually validated free-living marine nematode taxa (no. of reference sequences = 18991, no. of nematodes reference sequences = 971; database retrieved from: Macheriotou et al. (2019); Macheriotou et al. (2020). The taxonomic information and the environmental parameters were then stored in phyloseq (McMurdie and Holmes, 2013) or ampvis2 (Andersen et al., 2018) format unless the analysis required a specific alternative data input. All the ASVs detected in the extraction negative and PCR negative controls were removed. The ASV table was then rarefied to the lowest sequencing counts and singletons were removed. The rarefaction curves were plotted to ensure that all samples reached a diversity plateau. All ASVs that did not receive a taxonomical assignment at Kingdom level were removed from the dataset.

2.5. Community composition and diversity analyses

The community compositions of all metazoans were plotted by transforming the corresponding ASVs read counts into relative abundance. For the Nematoda relative abundance, we only used the reads from the ASVs assigned to Nematoda (rarefied total reads = 630 000, nematode filtered reads = 63 809). The alpha-diversity indices (observed richness for genus and ASVs level) were computed using the R package phyloseq, according to the nine sampling habitats. Pairwise permutation test (n = 1000) and Bonferroni correction were used to indicate significant differentiation among sampling locations. The NMDS plots of the nematode communities were computed using the R package ampvis2, using Bray-Curtis dissimilarity distance of the nematode communities in each sequencing replicates (Somerfield, 2008). To validate the grouping rationale of the nematode communities in AT, the Bray-Curtis distance for northern slope and southern slope against stations at the trench axis were compared. T-test was used for statistically significant differentiation.

2.6. Environmental factors correlation and co-occurrence modules analyses

PCA was used to investigate sampling regions structuring according to environmental conditions by Euclidean distance matrix. R package Envfit was used to estimate the linear explanatory relation of selected environmental factors on the PCA. The same R package was also used for the linear explanatory relation of the filtered environmental factors with nematodes communities using RDA. Pseudo-F and significance level of the RDA was computed with permutation test (n = 1000). A co-occurrence network was computed to inspect the significance between co-occurring nematode ASVs using the R package SpiecEasi (settings: method = glasso, lambda.min.ration = 1e-1, nlambda = 100, rep.num = 20 and thresh = 0.2) (Kurtz et al., 2015), and only the positively co-occurring edges from the network were selected. R package igraph was used in module detection and clustering with Louvain algorithm (Csardi and Nepusz, 2006). Each module's relative abundance in the sampling locations, and their correlation with the filtered environmental factor were statistically examine using the R package WGCNA (Langfelder and Horvath, 2008).

2.7. Metaphylogeography analyses

Shared nematode genera and ASVs across sampling locations were examined using the R package ComplexUpset (Krassowski, 2020). The ASVs sequences and respective counts of the nematode genera *Halalaimus* de Man, 1888 (Hal), *Chromadorita* Filpjev, 1992 (Chr), *Desmoscolex* Claparède, 1863 (Des), *Acantholaimus* Allgen, 1933 (Aca), *Molgolaimus* Ditlevsen, 1921 (Mol), and *Oxystomina* Filipjev, 1918 (Oxy) were extracted from the phyloseq object. To minimise potential artifacts from read counts variation in our samples, only sampling habitats with more than 50 reads in all ASVs belonging to these genera were kept. The filtered reads counts were transformed into five semiquantitative index ranks as described in Turon et al. (2020) and then used for population-structure analysis. Haplotype-based pairwise Fst calculations were computed using the R packages hierfstat, with permutation test (n = 1000) performed and Bonferroni correction applied for p-value correction to distinguish significant genetic differentiation among populations (Goudet, 2005; Mehta et al., 2019). For haplotype network, the ASVs sequences belonging to the same genus were aligned using Clustal-W

v.2.0 (Larkin et al., 2007) under default settings. The reads counts information were visualised in POPART v1.7 (Leigh et al., 2015) with a median-joining network algorithm. Lastly, the percentages of haplotypes found across the two trench systems, within one trench, and unique haplotypes, together with the corresponding read counts were also summarised.

The bioinformatic scripts for data handling and processing for this study are available on the GitLab Page (https://hadal.pages.sdu.dk/nematodes_edna). This includes all self-written computational scripts and R scripts for the analysis and will be publicly available upon publication for the reader's information.

3. Results

3.1. Overall sequencing results

All nine sampling habitats had at least one successful sequencing replicate, totalling 28 amplicon sequencing data from 15 stations. The 28 rarefied samples generated a total of 5991 ASVs, and the rarefaction curve from each sample documented that successfully sequenced samples reached diversity plateau (Supplementary Fig. 1). When excluding all of the Kingdom-level unclassified ASVs, 4240 (70.8 %) could be classified with an eukaryotic origin, of which 1356 (22.6 %) ASVs could be taxonomically assigned to Metazoan (40.0 % of all sequencing reads). Phylum Nematoda was the majority of these phylum-assigned ASVs (16.1 % of all sequencing reads) across the samples, where relative abundance varied from 88.9 % to 6.7 % in different replicates. The highest relative abundance of Nematode ASVs was detected in PS133/

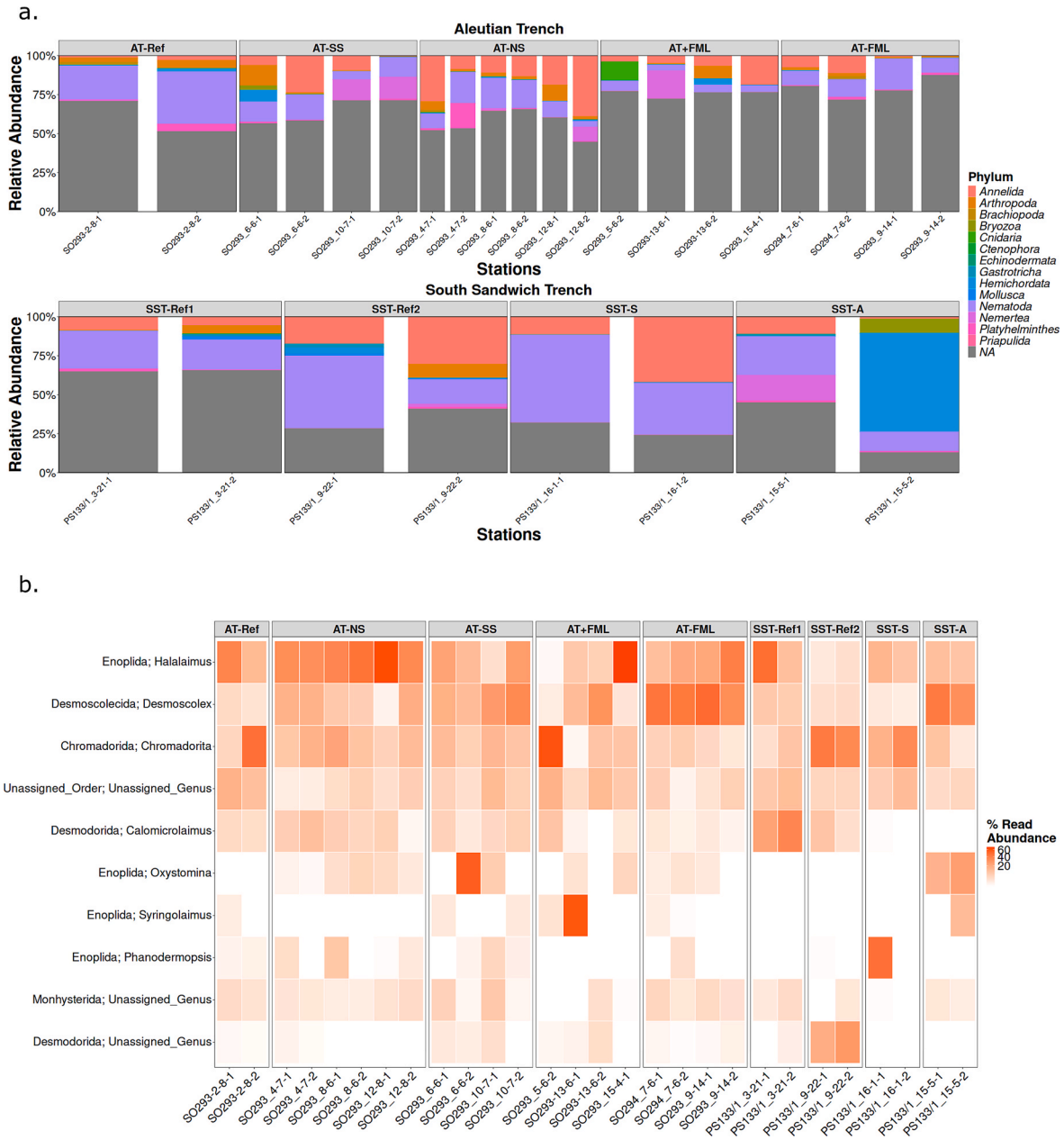

Fig. 2. The relative abundance of metazoans ASVs and nematode ASVs detected in this study. 2a. The relative abundance of metazoans ASVs reads. All of the single-cell eukaryotes assigned ASVs were excluded. Each bar represents one sequencing replicate. **2b.** Heat-map for the relative abundance of Nematoda ASVs (y-axis: Family; Genus). Each column represents one sequencing replicate. Only the top 10 most abundant nematodes genera are shown.

1_16-1–1 (SST-S) and lowest was detected in SO293_13-6–1 (AT+FML) (Fig. 2a).

For nematodes, a total of 979 ASVs were obtained (72.2 % of all metazoans; 16.3 % of all identified ASVs) and were used in all downstream bioinformatic analysis. Within the nematode ASVs, 297 ASVs (30.3 %) were not able to be resolved at species level with the current taxonomical database, resulting in 682 ASVs that were assigned to species level as highest taxonomical rank. These ASVs belonged to 58 genera, and only 4 genera were detected across all stations (Supplementary Fig. 3). *Halalaimus* was the most abundant genus and was detected in all sequencing replicates, consisting of an average relative abundance of 33.7 %, where the highest occurrence 68.7 % appears in SO293_15-4–1 (AT+FML) and lowest occurrence of 0.3 % in SO293_5-6–2 (AT+FML). Aside from this exception, the relative abundance of *Halalaimus* did not show great differences among stations in the AT sampling habitats and was two times higher in the overall AT sampling habitats (average of 28.6 %) than the overall SST sampling habitats (average of 14.3 %). The variation of *Halalaimus* relative abundance was more apparent in the SST sampling habitats with highest relative abundance of PS133/1–21-1 at SST-Ref1, while a minimum relative abundance of *Halalaimus* was encountered at both replicates in PS133/1_9-22 at SST-Ref 2. Relative abundance of *Desmoscolex* was two times higher in AT sampling habitats than in SST sampling habitats (an average of 18.2 % in AT compare to 9.3 % in SST, respectively). In both trenches, the occurrence of *Desmoscolex* increased with water depth with average relative abundances of: 6.1 % at reference sampling habitats; 11.0 % at slope sampling habitats; and 25.1 % in trench axis sampling habitats. The third most abundant genus, *Chromadorita* had highest relative abundance in SO293_5-6–2 (AT+FML). It was found most abundant in AT+FML in AT and in SST-Ref1 in SST, but with lower relative abundance in SST in general. The average relative abundance of *Chromadorita* did not differ much between the two trenches (15.9 % and 19.5 %, in AT and SST regions, respectively) (Fig. 2b).

When comparing the relative abundance of nematodes within AT slopes sampling habitats, the nematode composition in the AT-NS stations was associated with higher relative abundance of *Halalaimus,* while in AT-SS the relative abundance of *Halalaimus* and *Desmoscolex* were similar to each other. *Syringolaimus* de Man, 1888 was also only found in the AT-SS but not in AT-NS. When comparing between AT+FML and AT-FML, the composition in the stations of AT-FML were more homogenised, both stations and replicates suggesting a similar relative abundance of nematode genera in general. While in AT+FML, each replicate and station had a different dominating genera according to the highest relative abundance, suggesting the heterogeneity of nematodes composition in this sampling habitat. In SST, the variation between the replicates of stations was less. Yet, the dominating genus in each sampling habitats in SST was distinct. Overall, although the nematode composition occasionally varied among replicates within each station and between stations within the same habitat, the relative abundance and composition of nematodes were generally distinct across the different sampling habitats (Fig. 2b).

3.2. *Nematodes communities structure and correlation with environmental data*

The NMDS analysis of nematode communities showed a distinct clustering of most sampling habitats, based on Bray-Curtis dissimilarity (Fig. 3). The only exception was the overlapping of AT-NS and AT-SS. This implies that the sampling habitats among the two trenches host distinct nematode communities. Furthermore, the inter comparison of Bray-Curtis dissimilarity for AT-SS and AT-NS indicated the slope sampling habitats in AT were not significantly differentiated in terms of nematode communities (Supplementary Fig. 2). The overall alpha diversity for observed ASVs richness and observed genera richness expressed no significant difference between the nine sampling habitats (Supplementary Fig. 4). The PCA that was constructed only using the benthic environmental conditions in the sampling habitats, indicated a clear separation between AT and SST, differences that apparently were statistically related to microbial abundances, TN and TOC content (Fig. 4a). In AT, TOC and TN content further separated the groupings into stations with and without FML. At the SST, the four habitats were mainly separated by the sand and silt content.

According to correlation between environmental parameters, sand and clay were excluded for the RDA analysis since they were highly correlated with other variables. (Supplementary Fig. 5). The RDA plot provided an overall significant correlation (Pseudo-F: 1.73, p-value 0.001), and microbial abundances were the major factor for an overall separation across the nine sampling habitats at AT and SST (Fig. 4b). However, SST-Ref1 and AT+FML were clustered closer with both AT-NS and AT-SS on the RDA, suggesting the variance between the nematode

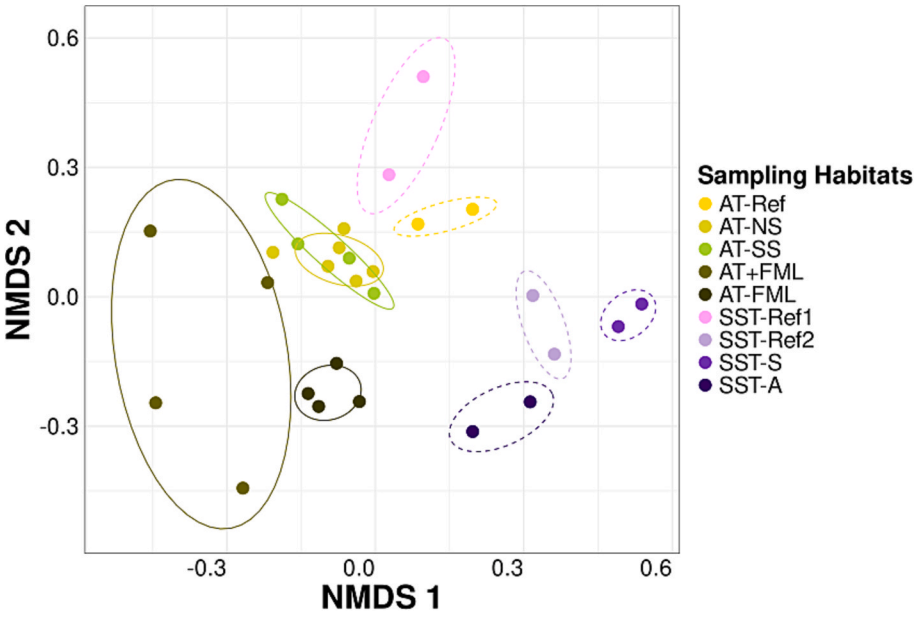

Fig. 3. NMDS and sampling-location clustering. The NMDS plots clustered by the Bray-Curtis dissimilarity of the nematode communities (NDMS stress-level = 0.21; n = 28). Solid-lined ovals indicate the confidence eclipsing (n > 2), dash-lined ovals indicate no confidence eclipsing due to small sample size (n = 2).

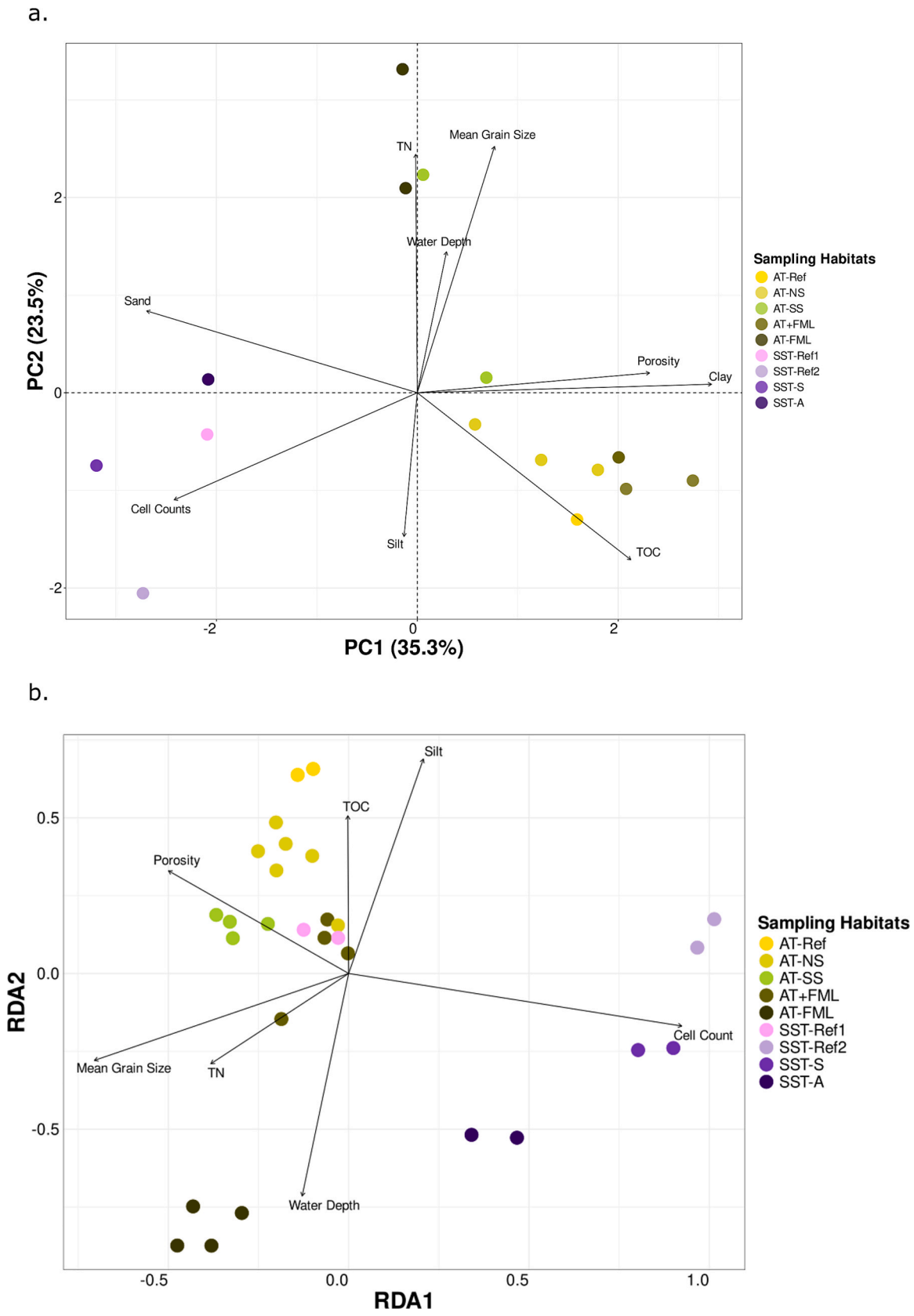

Fig. 4. Environmental correlation plots indicating the correlation of environmental factors and the clustering of the sampling location. 4a. The PCA correlation of sampling habitats according to environmental parameters. (n = 15) **4b.** The RDA conducted following filtering of correlated environmental factors and nematodes ASVs reads. (n = 28, RDA Pseudo-F: 1.73, p-value = 0.001).

communities in these sampling habitats were influenced by similar environmental factors. For AT-FML, water depth became the primary environmental parameter that separate these stations from all other sampling habitats.

3.3. Shared nematodes genera and co-occurring nematodes correlations with environmental factors

A large number unique nematodes ASVs (n = 812) were found across all sampling habitats (Supplementary Fig. 6). There were also no shared ASVs across all sampling habitats. When considering shared nematodes genera, four genera were found to be shared across all sampling habitats (Supplementary Fig. 7). No unique genera were found in AT+FML and SST-A, while the other sampling habitats had a total of nine genera that were unique to a single sampling habitat. Overall, a high proportion of nematodes genera (n = 50) were found shared across at least two sampling habitats.

Co-occurrence network and module analyses were conducted to investigate the correlations between potential environmental drivers and co-occurring nematode species (Fig. 5). Overall, the co-occurring nematode ASVs were classified into 15 different modules. These 15 modules were distributed across all sampling habitats, and none of them were unique to any single habitat. Moreover, there were also no module found dominating in more than one habitat (relative abundance > 50 %). However, module 3, 13 and 15 were restricted to AT, while no exclusive modules existed in SST. AT-Ref, AT-FML, SST-Ref1, SST-Ref2, SST-S and SST-A were composed by more than 50 % of module 4, 7, 8, 9, 1 and 2 respectively. SST-A was also found to have the least module composition with only 5 modules. For AT-NS and AT-SS, they almost shared the same module composition, except module 9 which was only found in AT-NS. For the taxonomical composition of modules, *Desmoscolex* was the most common genera present in every module, which was distinctly clear in module 9 with more than 50 % of relative abundance. *Halalaimus* and *Chromadorita* were the second and third most common genera, with the highest relative abundance in module 8 and module 2, respectively. Module 4 was composed of most unique taxa, *Diplolaimelloides* Meyl, 1954, *Praeacanthonchus* Micoletzky, 1924 and *Anticoma* Bastian, 1865 were only found here (Supplementary Fig. 8). When examining the correlation of environmental factors with modules, modules 3, 5, 6, 8, 13 and 14 had no significant correlation with any of the environmental factors. Only module 2 was found to correlate with two environmental factors, positively with water depth, and negatively with porosity. Although TOC content had no significant correlation with any of the modules, other factors may mediate its influence on nematodes. Microbial abundance (indicated as cell counts in Fig. 5) were positively correlated with modules 1, 9 and 12, while TN content was positively correlated with modules 10, 11 and 15. These correlations with multiple modules possibly indicated food availability and food quality were critical in assembling the nematode community.

3.4. Metaphylogeography analysis for dominating genera

The population structure and potential connectivity of the six dominating genera in the nine sampling habitats were examined with haplotype network (Fig. 6a—6c), haplotype-based pairwise Fst with corrected p-values (Supplementary Table 3–8) and the percentage of shared and unique haplotypes with percentage of assigned reads (Table 2).

For *Halalaimus* and *Desmoscolex*, the genetic diversity was the highest among the six genera of interest, with 134 and 163 haplotypes found, respectively. There were 8.2 % and 4.3 % of shared haplotypes found across and within trenches. The pair-wise Fst values for both genera were low in general (<0.1) and mostly not significantly different. However, significant differentiation between some populations were found, both within habitats in the trench and across the two trenches. We observed that shared haplotypes were found within and between trenches. The unique haplotypes found in one habitat did not cluster together in their respective networks, but instead originated from haplotypes that were undetected in the same habitat. Additionally, the comparatively low number of mutational differences between

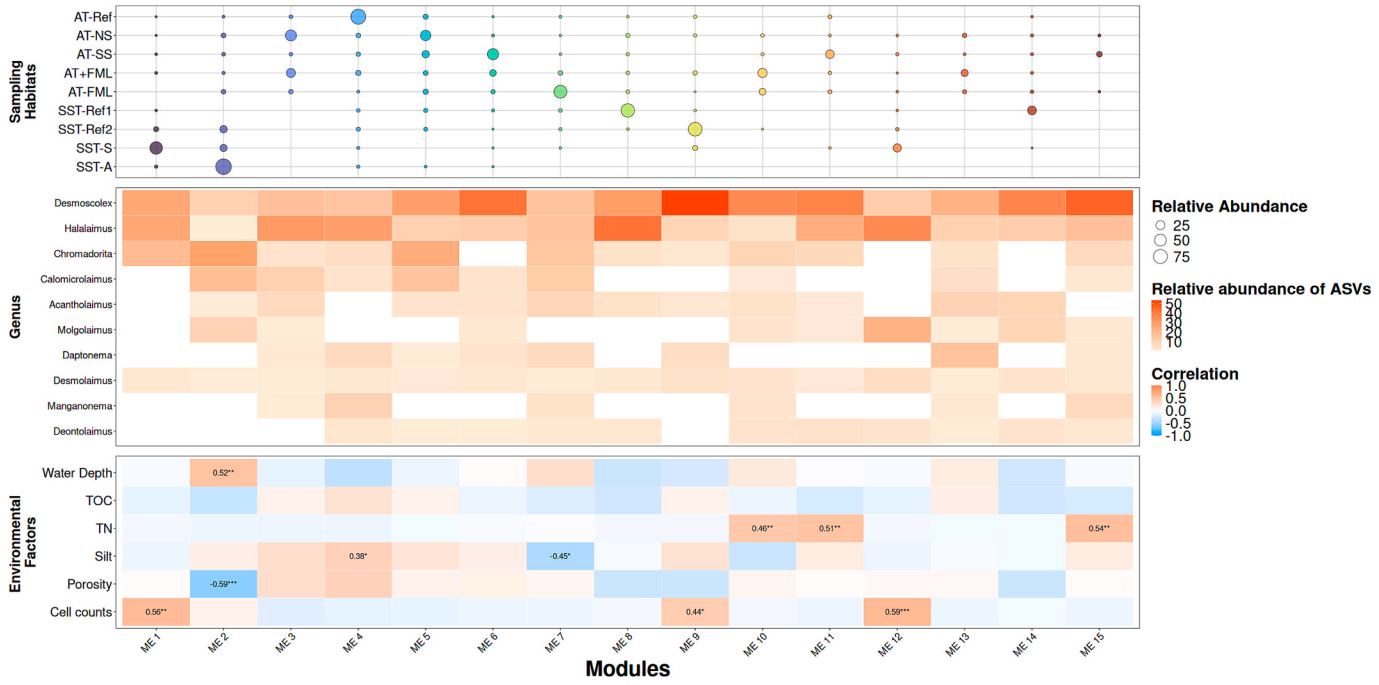

Fig. 5. Co-occurrence network modules analysis. **Upper panel.** The module clustering of the co-occurring ASVs across all sampling habitats. Relative abundance of each module represented by the size of the circle. **Mid panel.** Heat map of taxonomical composition of each clustering module. Each column represents a module and y-axis representing the genus of the nematodes and the relative abundance were grouped in genus level. Only top 10 most abundance nematode genera were shown. **Lower panel.** Heat map of the positive (red) and negative (blue) correlation of environmental factors towards each module. Only significant value (p-value < 0.05) are illustrated, the level of significance is indicated with * in the plot. Y-axis representing the environmental factors.

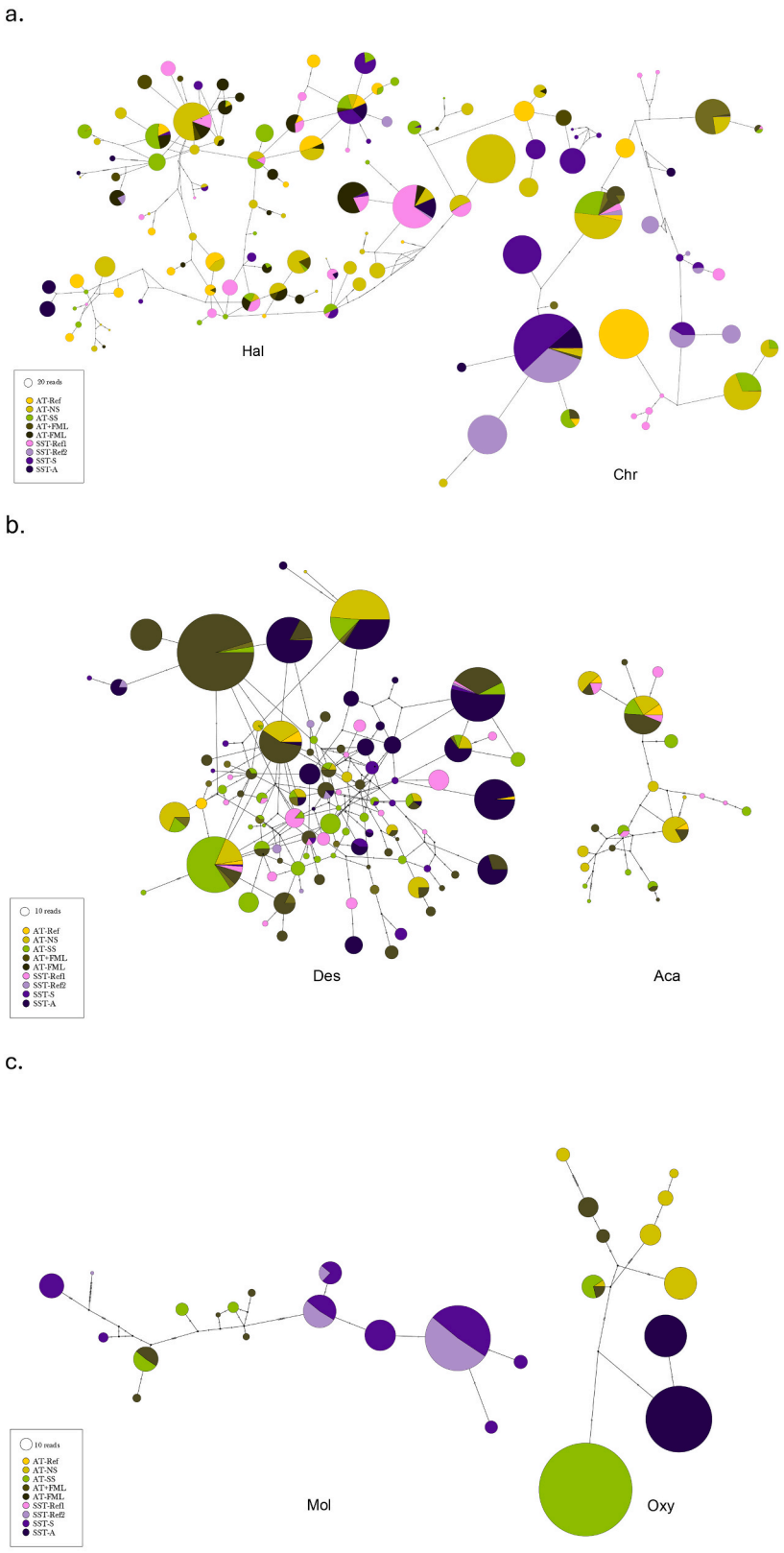

Fig. 6. The haplotype-network plot of the six **nematode genera of interest**. **6a.** Network of Hal and Chr. **6b.** Network of Des and Aca. **6c.** Network of Mol and Oxy. Each pie represent a haplotype found on the 18S marker gene after minimal reads filtering. The size of the pie represent the read numbers associated with the particular haplotype. The colour code indicates the sampling location of and the reads counts detected.

Table 2
The percentage and total number of shared and unique haplotypes, between and within trench(es) respectively, and the associated read counts of the six nematode genera of interest after minimal reads filtering.

Genus	Shared haplotypes between trenches		Shared haplotypes within trench		Unique haplotypes		Total	
	% of haplotype	% of reads	% of haplotype	% of reads	% of haplotype	% of reads	Haplotype	Reads
Hal	8.2	20.9	11.2	17.8	80.6	61.3	134	14,210
Des	4.3	24.4	5.5	22.3	90.2	53.3	163	7835
Chr	13.8	44.6	20.7	16.4	65.5	40.0	29	10,891
Aca	14.3	55.4	9.5	19.9	76.2	24.7	21	858
Mol	0	0	25.0	72.3	75.0	22.7	16	1612
Oxy	0	0	9.1	3.0	90.9	97.0	11	3195

haplotypes indicated that their evolutionary history has not created large genetic divergence between haplotypes. These observations indicated an intermediate degree of connectivity between the populations within and across trenches.

The connectivity of *Chromadorita* was potentially stronger compared to *Halalaimus* or *Desmoscolex*. The Fst values of *Chromadorita* between populations were not significantly differentiated, except between SST-A and other habitats (pairwise Fst value for SST-A to others: >0.1). The overall genetic diversity was also lower, only 29 haplotypes were found. Together, these results suggested the population connectivity within and across trenches for this genus was more substantial, except for the populations in SST-A. *Acatholaimus*'s connectivity dynamics might be similar but potentially weaker to the *Chromadorita* since 14 % of shared haplotypes were found, low Fst values (<0.1) and significant differences were only found between AT-SS and AT-FML.

For *Molgolaimus*, the connectivity of this genus may be limited within trenches and with no connectivity across trenches, resulting in localized connectivity within a trench system only. Since only four haplotypes were shared, Fst values were high (>0.1) and the pairwise comparison indicated significant differences between all population. In *Oxystomina*, connectivity was very low between populations across the sampling habitats. None of the haplotypes were found shared between trenches and 90 % of them were found to be uniquely in one habitat. The SST-A population was significantly different from the AT populations, and the genetic diversity in SST was extremely low since only two haplotypes were found. Within AT, Fst comparison revealed no significant differences but in fact only one haplotype was shared, which may have been an artifact from the low statistical power for this genus. Overall, the metaphylogeography analysis reflected the genetic diversity and suggested different connectivity dynamics of hadal nematode populations within and across trenches.

4. Discussion

It is challenging to recover full benthic metazoans biodiversity in sediments using eDNA metabarcoding approaches (Dell'Anno et al., 2015). Yet, the amplicon sequencing results obtained from this study reveal the nematode-diversity patterns in AT for the first time. In general, results can be compared with other previous diversity analyses based on classic taxonomical investigations both in the abyssal deep sea and in hadal trenches (Cordier et al., 2022; Lejzerowicz et al., 2021). In most samples, Nematoda is the most dominating eukaryotic phylum. The relative abundances were, however, lower than previously reported values of hadal studies that were based on morphological traits. Here the relative abundance of nematodes accounted for >90 % of the benthic community (Leduc et al., 2016). A possible explanation is the fact that deep-sea sediment itself represents an ideal environment for preserving eDNA which might originate from segment or body parts of deposited organism from the surface water (Lejzerowicz et al., 2013; Rivera Rosas et al., 2024). Microbial DNA in the sediment would also be amplified alongside with the nematodes DNA, thereby reducing the relative nematodes ASVs being detected (Hugerth et al., 2014). Such eDNA fragments also contribute to the large proportion of ASVs that could not be taxonomically assigned at phylum level. We do not expect that unassigned ASVs represent new phyla, but rather attributable to incomplete genetic and morphological baseline data of the deep-sea benthos (Cordier et al., 2022). Yet, the benthic communities at great water depths are dominated by meiofauna, and especially dominated by the phylum Nematoda (Zeppilli et al., 2018).

The dominating nematode genera detected in our data were also reported as common genera in other trench systems and their adjacent deep-sea habitats, such as in Tonga Trench, Atacama Trench and Kermadec Trench (Gambi et al., 2003; Horacek III et al., 2022; Leduc and Rowden, 2018; Leduc et al., 2016). However, most of the available studies were based on morphological approach and hence lack the genetic information to directly compare with our metabarcoding results. Thus, our discussion focuses on metabarcoding data for characterizing and investigating nematode communities in the two hadal trench systems under the framework of *the meiofauna paradox*. As inspired by Giere (2009), the following sections split the paradox into two questions: 1) Is every habitat in the trenches different? and 2) could some haplotypes be everywhere in the trench?

4.1. Every habitat in the trenches is different

The Aleutian Trench and South Sandwich Trench harbour distinct hadal habitats with different environmental conditions. The two trench systems are located in different hemispheres and in two different oceans, the North Pacific Ocean and the South Atlantic Ocean. The contrasting environmental conditions are shaped by differences in surface-ocean productivity, seafloor bathymetry and depositional dynamics all resulting in different benthic biogeochemical environments. As expressed by the NMDS clustering, the nematode-community composition is also very different when comparing sampling habitats. However, one exception is that the communities are similar in AT-NS and AT-SS despite these two habitats exhibiting differences in environmental conditions. Given the lack of mobility of nematodes, we expected that the FML at the AT trench axis, which is anticipated to be a hostile environment for metazoans (Sindlev et al., 2025), would present a spreading barrier for nematodes. Remarkably, the nematodes appear to be capable of colonising both slopes of AT, despite the FML barrier along the trench axis. These observations could be due to selective pressure or the presence of nematodes that have adapted to similar environments despite being separated, or, to a lesser extent, the lack of taxonomic species level resolution.

Similar environmental factors contributing to the close clustering of AT+FML, SST-Ref1 and AT slopes habitats in the RDA analysis was unexpected. The clustering could imply that microbial abundances, which indicate nematode food availability and quality, could be a key driver in shaping nematode diversity in the deep sea (Shimabukuro et al., 2022) and overrule the importance of other environmental factors such as water depth or sediment texture. When food supply is limited, population size, genetic exchange, and ecological interactions become restricted due to the insufficient nutritious-energy supply (Herman and Vranken, 1988; Moens and Vincx, 2000; Sibly and Calow, 1983). A similar observation is evident in our AT-Ref sampling habitats, where

microbial abundances are relatively low. When food availability or food quality is elevated, as reflected by the increased microbial abundances in our dataset, environmental factors seems to affect distinct habitats more similarly (e.g., AT slopes and SST-Ref1). With more food available supporting larger population sizes, greater reproductive activity is feasible, possibly accompanied by a higher frequency of genetic exchange or mutation events (Dos Santos et al., 2008; Jiang et al., 2010; Moore, 1979). This can enhance genetic diversity, which, over time, promotes higher species diversity within the ecosystem. The nematode communities in the hadal trench habitats presumably originate from the seafloor plains and are transported by passive dispersal into these habitats, as described by Ptatscheck and Traunspurger (2020). However, when food becomes abundant and the quality is elevated at the trench axes, habitat-specific communities may emerge. As discussed in McPeek (1996), speciation, promoted by niche partitioning, could also shape distinct communities that are specific to each habitat. This is reflected in the communities of SST-Ref2, SST-S, and SST-A, which were characterised by high food availability. However, the effect of environmental filtering might be critical, as seen in AT-FML, where microbial abundances were similar to AT slopes habitats but not at hadal water depth. The nematode communities here remained distinct from communities at other habitats. Furthermore, the clustering of AT+FML could suggest that when food availability and quality decline, community composition may also be reverted back to a nutritious-limited community structure. Our results would suggest that each trench harbours their own habitat specific nematode community primarily driven by availability and quality of food and subsequent environmental filtering.

To further investigate the specific environmental drivers that may explain the dissimilarity of community composition in these nine habitats, we explored the correlation of the environmental factors with co-occurring nematode modules. The absence of any single module dominating in more than two habitats implied that the nematode community are specific to given habitats. A ubiquitous nematode community for trenches (or related habitats) does not exist. Our genetic data confirm that the habitats in each trench system host unique nematode assemblages, supporting the observation that nematode community composition can differ markedly even between adjacent trench systems as shown with morphology by Leduc and Rowden (2018). The TOC content has no correlation with any of the clustered modules. It has previously been argued that rather than TOC content, the TOC-quality, as expressed by activity and biomass of microbes, better defines favourable habitats for deep-sea nematodes (Shimabukuro et al., 2022). Although we did not directly measure microbial activity in the sediment, microbial abundance and TN content each displayed a strong positive correlation with three distinct modules. There appears to be only a minor correlation between water depth and community structure, suggesting that hydrostatic pressure plays a relatively limited role in shaping hadal nematode communities directly. A substantial proportion of modules showed no correlation with any of the measured environmental parameters, suggesting that other, as yet unexplored, ecological drivers may be influential. Potential factors could include seafloor topography, bottom currents, episodic or mass wasting deposition events that passively transport nematodes into the trench, or trophic interactions such as consumer-mediated processes (Duffy, 2002; Zajac, 2008; Zeppilli et al., 2016). While the overall taxonomic composition at the genus level appeared relatively consistent across habitats, the lack of clear associations with individual environmental factors suggests that stronger environmental filtering likely occurs at the species level. The heterogeneity of deep-sea environments may favour endemic speciation, indicating that each habitat supports a distinct community composition.

4.2. Some haplotypes could be everywhere in the trench

Some nematode genera, including *Halalaimus*, *Desmoscolex* and *Chromadorita* are widespread and dominant across the two trenches. These three genera are found in every module with high relative abundances (in top 10 of all genera), albeit they cannot be classified into an individual module. In systematic investigations these deep-sea genera are often considered as widespread (and cosmopolitan) (Leduc and Rowden, 2018; Leduc et al., 2016; Vanhove et al., 2004; Vanreusel et al., 2010), and our findings suggest that these genera may exhibit an enhanced ability to tolerate diverse deep-sea environments. For instance, *Halalaimus* appears to have undergone multiple invasion events between shallow and deep-sea habitats over the course of its evolutionary history (Bik et al., 2010). These findings also indicate that each nematode species may exhibit different levels of resilience towards different environmental selection pressures. In addition to the shared haplotypes found across all sampling habitats, a substantial proportion of unique haplotypes was identified. This aligns with the observation of many habitat-specific ASVs, suggesting that the genetic diversity within the source populations from the seafloor plains—or the broader metacommunity—is already considerable (Leibold et al., 2004). When passive dispersal occurs, the population are transported into new habitats, for example from the seafloor plains to the slope or even into the trench axis. The population is likely to experience new environmental filtering and selective pressures due to shifts in environmental conditions (Macheriotou et al., 2023). For species with limited resilience capacity to new selective forces, less resilient individuals (or haplotypes) will presumably be eliminated, leaving only the resilient individuals (or haplotypes) to survive in the colonized environment. Meanwhile, the population in the new environment becomes isolated again. Over evolutionary timescales, these resilient individuals are adapted to the new conditions and reproduce, resulting in an apparent reduction in connectivity with the original source population. Conversely, species with higher resilience capability experience weaker selective pressure, allowing them to survive, colonise and reproduce in new habitats. This maintains genetic diversity within the population and reflects higher connectivity with the source population. It is also important to consider that nematodes are very small and lack long-distance mobility, making active dispersal unlikely (Derycke et al., 2013; Ptatscheck and Traunspurger, 2020). Therefore, environmental filtering is likely the most critical factor shaping their population structure in hadal trench environments.

The observed variation in genus-connectivity presumably reflect variations in adaptability among the genera or even on species level. The connectivity on another meiobenthic taxon, single-celled foraminiferan species has also demonstrated gene flow between distant populations in the Antarctic and the Arctic (Darling et al., 2000). A more mobile hadal macrofaunal amphipod species, *Alicella gigantea* Chevreux, 1899, has been suggested to exhibit gene flow between distant trenches spanning half of the global ocean (Maroni et al., 2025). In contrast, other amphipod species, such as *Paralicella* Chevreux, 1908 (RFLP species 2), display a more restricted distribution with only marginal gene flow between trench systems (Ritchie et al., 2017). Similar species-level variation could be evident in our study. For example, genera like *Halalaimus*, *Desmoscolex*, *Chromadorita* and *Acantholaimus* have greater adaptability to diverse deep-sea environments, as indicated by the observed connectivity patterns. Conversely, *Molgolaimus*, and *Oxystomina* appear to exhibit lower environmental adaptability, reflected in large proportions of localized haplotypes. Since most nematode dispersal is passive, some nematode population may successfully endure environmental stresses during sequential long-distance transport and colonize different habitats. Therefore, hadal trenches should be viewed as dynamic regions connecting adjacent habitats by dispersal of nematode populations. It is essential to examine nematode population structures and connectivity on a species-by-species basis. Our results provide evidence that some nematode haplotypes are present across multiple habitats due to their high resilience capacity to varying environments, even in extreme settings such as hadal trenches.

The population structure of hadal nematodes examined in this study may be either overestimated or underestimated due to the gene copy number variations, intragenomic polymorphisms, PCR bias and the

relatively short and conserved 18S ribosomal DNA gene fragment used (Ahmed et al., 2019; Liu et al., 2022; Pereira et al., 2020; Tang et al., 2012). Combining multiple gene markers (e.g. COI, 28S or ITS) for metabarcoding could enhance our understanding of nematode-diversity patterns and distribution, provided the existence of comprehensive reference databases (Gielings et al., 2021). However, establishment of such databases for meiofauna is still limited and requires additional sampling and sequencing effort. Given the lack of an adequate reference database, inclusion of an additional gene marker would likely not improve the resolution on genetic diversity in our study—as we observed with a COI marker—and hence these data were not further considered. Thus, the 18S marker remains a preferable choice due to its wide taxonomic coverage and reliable reference database for deep-sea nematodes (Charrier et al., 2024). Nonetheless, our results demonstrate that community composition correlates with various environmental drivers, supporting its use as a proxy for population structure in investigating the meiofauna paradox through molecular insights. Most importantly, there is a pressing need to develop and apply more advanced molecular tools—such as mitochondrial or whole-genome sequencing—on individual deep-sea nematode specimens, alongside traditional morphological methods, to better understand how hadal trenches are connected to the global ocean ecosystem.

5. Conclusion

Sequencing techniques are powerful tools for uncovering deep-sea meiofaunal diversity. In this study, we employed a metabarcoding approach to investigate the distribution and connectivity of nematode genera across two distant trench systems. Our analyses reveal that nematode communities in the Aleutian and South Sandwich trenches are distinct and endemic, likely driven by differences in food availability, food quality and other environmental factors. However, certain shared nematode haplotypes were found in both trench systems, indicating some degree of connectivity and no clear evidence of geographic isolation. These findings provide the first molecular evidence supporting the meiofaunal paradox in the hadal realm: while communities differ everywhere, some taxa are indeed found everywhere.

6. Data statement

All faunal data analysed in this study are available as part of the main document or Electronic Supplement.

Funding credit

The AleutBio project was funded by the PTJ (German Ministry for Science and Education), grant 03G0293A to Prof. Dr. Angelika Brandt, Senckenberg Research Institute and Natural History Museum as well as Goethe University, Frankfurt, Germany.

This work is financially supported by the Danish National Research Foundation grant DNRF145, rewarded to Prof. Dr. Ronnie N. Glud, via the Danish Center for Hadal Research (HADAL).

CRediT authorship contribution statement

Yick Hang Kwan: Writing – review & editing, Writing – original draft, Methodology, Investigation, Data curation, Conceptualization. **Sofie Derycke:** Writing – review & editing, Supervision, Investigation, Conceptualization. **Blandine Trouche:** Writing – review & editing, Investigation, Conceptualization. **Frank Wenzhöfer:** Writing – review & editing, Funding acquisition, Data curation. **Mathias Middelboe:** Writing – review & editing, Data curation. **Angelika Brandt:** Writing – review & editing, Investigation, Funding acquisition, Data curation, Conceptualization. **Mauricio Shimabukuro:** Writing – review & editing, Supervision, Investigation, Conceptualization. **Ronnie N. Glud:** Writing – review & editing, Writing – original draft, Supervision, Project administration, Funding acquisition, Data curation, Conceptualization. **Daniela Zeppilli:** Writing – review & editing, Writing – original draft, Supervision, Methodology, Investigation, Conceptualization.

Declaration of competing interest

The authors declare that they have no known competing financial interests or personal relationships that could have appeared to influence the work reported in this paper.

Acknowledgements

We would like to thank the master, crew, and participants of the RV Sonne expedition SO293 (AleutBio) and RV Polarstern expedition PS133/1 (cruise leader C Klaas) for their assistance on board. Ship time for PS133/1 was partly provided under the secondary user grant GPF 20-2_024, South Polar Carbon to F.W. and R.N.G. Our appreciation also goes to all the student helpers and technicians who prepared the instruments and supported and helped sorting the extensive expedition material or helped with data measurements and/ or data acquisition. AleutBio is endorsed by UNESCO (No. 59.2) as part of the UN Decade of Ocean Science for Sustainable Development 2021-2030, and it contributes to the UN Project Challenger 150. We would also like to express our gratitude to the editors and anonymous reviewers for their helpful comments and suggestions.

Daniela Zeppilli was supported by the project "Massive mEIOfauna DiscoverY of new Species of our oceans and SEAs (MEIODYSSEA) funded by the Ocean Shot Research Grant Program of the Sasakawa Peace Foundation, supported by the Nippon Foundation.".

This is AleutBio publication # 30.

Appendix A. Supplementary data

Supplementary data to this article can be found online at https://doi.org/10.1016/j.pocean.2025.103594.

Data availability

All measurement data were available in the Supplementary Information provided. High-throughput sequencing data were available on European Nucleotide Archive (ENA) at EMBL-EBI under accession number PRJEB94967. They will also be deposit in public databased, and will be publicly available upon publication.

References

Ahmed, M., Back, M.A., Prior, T., Karssen, G., Lawson, R., Adams, I., Sapp, M., 2019. Metabarcoding of soil nematodes: the importance of taxonomic coverage and availability of reference sequences in choosing suitable marker (s). Metabarcoding and Metagenomics 3, e36408.

Andersen, K.S., Kirkegaard, R.H., Karst, S.M., Albertsen, M., 2018. ampvis2: an R package to analyse and visualise 16S rRNA amplicon data. *BioRxiv*, 299537.

Bao, R., Strasser, M., McNichol, A.P., Haghipour, N., McIntyre, C., Wefer, G., Eglinton, T. I., 2018. Tectonically-triggered sediment and carbon export to the Hadal zone. Nat. Commun. 9 (1), 121.

Bik, H.M., Thomas, W.K., Lunt, D.H., Lambshead, P.J.D., 2010. Low endemism, continued deep-shallow interchanges, and evidence for cosmopolitan distributions in free-living marine nematodes (order Enoplida). BMC Evol. Biol. 10, 1–10.

Blankenship-Williams, L.E., Levin, L.A., 2009. Living deep: a synopsis of hadal trench ecology. Mar. Technol. Soc. J. 43 (5), 137–143.

Blaxter, M.L., De Ley, P., Garey, J.R., Liu, L.X., Scheldeman, P., Vierstraete, A., Vanfleteren, J.R., Mackey, L.Y., Dorris, M., Frisse, L.M., 1998. A molecular evolutionary framework for the phylum Nematoda. Nature 392 (6671), 71–75.

Brandt, A., 2023. Master track of SONNE cruise SO293 in 1 sec resolution (zipped, 19.5 MB) (PANGAEA. https://doi.org/10.1594/PANGAEA.954247.

Brandt, A., Jażdżewska, A.M., Kaiser, S., Błażewicz, M., Gerken, S., Głuchowska, K., Kelch, A., Preikschardt, M., Knauber, H., Kohlenbach, K., 2025. Community composition and distribution of epi-and suprabenthic macrofauna in the bathyal, abyssal, and hadal zones of the northern North Pacific. Prog. Oceanogr. 230, 103376.

Callahan, B.J., McMurdie, P.J., Rosen, M.J., Han, A.W., Johnson, A.J.A., Holmes, S.P., 2016. DADA2: High-resolution sample inference from Illumina amplicon data. Nat. Methods 13 (7), 581–583.
Cerca, J., Purschke, G., Struck, T.H., 2018. Marine connectivity dynamics: clarifying cosmopolitan distributions of marine interstitial invertebrates and the meiofauna paradox. Mar. Biol. 165, 1–21.
Chan, J., Pan, B., Geng, D., Zhang, Q., Zhang, S., Guo, J., Xu, Q., 2020. Genetic diversity and population structure analysis of three deep-sea amphipod species from geographically isolated hadal trenches in the Pacific Ocean. Biochem. Genet. 58, 157–170.
Charrier, E., Chen, R., Thundathil, N., Gilleard, J.S., 2024. A set of nematode rRNA cistron databases and a primer assessment tool to enable more flexible and comprehensive metabarcoding. Mol. Ecol. Resour. 24 (5), e13965.
Cordier, T., Angeles, I.B., Henry, N., Lejzerowicz, F., Berney, C., Morard, R., Brandt, A., Cambon-Bonavita, M.-A., Guidi, L., Lombard, F., 2022. Patterns of eukaryotic diversity from the surface to the deep-ocean sediment. Sci. Adv. 8 (5), eabj9309.
Csardi, G., Nepusz, T., 2006. The Igraph Software. Complex Syst 1695, 1–9.
Darling, K.F., Wade, C.M., Stewart, I.A., Kroon, D., Dingle, R., Brown, A.J.L., 2000. Molecular evidence for genetic mixing of Arctic and Antarctic subpolar populations of planktonic foraminifers. Nature 405 (6782), 43–47.
Dell'Anno, A., Carugati, L., Corinaldesi, C., Riccioni, G., Danovaro, R., 2015. Unveiling the biodiversity of deep-sea nematodes through metabarcoding: are we ready to bypass the classical taxonomy? PLoS One 10 (12), e0144928.
Derycke, S., Backeljau, T., Moens, T., 2013. Dispersal and gene flow in free-living marine nematodes. Front. Zool. 10, 1–12.
Dos Santos, G., Derycke, S., Fonsêca-Genevois, V., Coelho, L., Correia, M., Moens, T., 2008. Differential effects of food availability on population growth and fitness of three species of estuarine, bacterial-feeding nematodes. J. Exp. Mar. Biol. Ecol. 355 (1), 27–40.
Duffy, J.E., 2002. Biodiversity and ecosystem function: the consumer connection. Oikos 99 (2), 201–219. https://doi.org/10.1034/j.1600-0706.2002.990201.x.
Fujii, T., Kilgallen, N.M., Rowden, A.A., Jamieson, A.J., 2013. Deep-sea amphipod community structure across abyssal to hadal depths in the Peru-Chile and Kermadec trenches. Mar. Ecol. Prog. Ser. 492, 125–138.
Gambi, C., Vanreusel, A., Danovaro, R., 2003. Biodiversity of nematode assemblages from deep-sea sediments of the Atacama Slope and Trench (South Pacific Ocean). Deep Sea Res. Part I 50 (1), 103–117.
Gerringer, M., Andrews, A., Huss, G., Nagashima, K., Popp, B., Linley, T., Gallo, N., Clark, M., Jamieson, A., Drazen, J., 2018. Life history of abyssal and hadal fishes from otolith growth zones and oxygen isotopic compositions. Deep Sea Res. Part I 132, 37–50.
Gielings, R., Fais, M., Fontaneto, D., Creer, S., Costa, F.O., Renema, W., Macher, J.-N., 2021. DNA metabarcoding methods for the study of marine benthic meiofauna: a review. Front. Mar. Sci. 8, 730063.
Giere, O., 2009. *Meiobenthology: the microscopic motile fauna of aquatic sediments*. Springer.
Giere, O., Schratzberger, M., 2023. *New horizons in meiobenthos research*. Springer.
Glud, R.N., Berg, P., Thamdrup, B., Larsen, M., Stewart, H.A., Jamieson, A.J., Glud, A., Oguri, K., Sanei, H., Rowden, A.A., 2021. Hadal trenches are dynamic hotspots for early diagenesis in the deep sea. Commun. Earth Environ. 2 (1), 21.
Glud, R. N., & Schauberger, C. (2024). Element cycling and microbial life in the hadal realm. *Trends in Microbiology*.
Glud, R.N., Wenzhöfer, F., Middelboe, M., Oguri, K., Turnewitsch, R., Canfield, D.E., Kitazato, H., 2013. High rates of microbial carbon turnover in sediments in the deepest oceanic trench on Earth. Nat. Geosci. 6 (4), 284–288.
Goudet, J., 2005. Hierfstat, a package for R to compute and test hierarchical F-statistics. Mol. Ecol. Notes 5 (1), 184–186.
Herman, P.M., Vranken, G., 1988. Studies of the life-history and energetics of marine and brackish-water nematodes: II. Production, respiration and food uptake by Monhystera disjuncta. Oecologia 77, 457–463.
Horacek III, H.J., Soto, E.H., Quiroga, E., Ingels, J., 2022. Meiofaunal nematode abundance, composition, and diversity at bathyal to hadal depths in the Southeast Pacific Ocean. Deep Sea Res. Part I 188, 103837.
Hugerth, L.W., Muller, E.E., Hu, Y.O., Lebrun, L.A., Roume, H., Lundin, D., Wilmes, P., Andersson, A.F., 2014. Systematic design of 18S rRNA gene primers for determining eukaryotic diversity in microbial consortia. PLoS One 9 (4), e95567.
Jamieson, A., 2015. *The hadal zone: life in the deepest oceans*. Cambridge University Press.
Jamieson, A.J., Fujii, T., Mayor, D.J., Solan, M., Priede, I.G., 2010. Hadal trenches: the ecology of the deepest places on Earth. Trends Ecol. Evol. 25 (3), 190–197.
Jamieson, A.J., Stewart, H.A., 2021. Hadal zones of the northwest Pacific Ocean. Prog. Oceanogr. 190, 102477.
Jiang, X., Mu, B., Huang, Z., Zhang, M., Wang, X., Tao, S., 2010. Impacts of mutation effects and population size on mutation rate in asexual populations: a simulation study. BMC Evol. Biol. 10, 1–13.
Kitahashi, T., Kawamura, K., Kojima, S., Shimanaga, M., 2013. Assemblages gradually change from bathyal to hadal depth: a case study on harpacticoid copepods around the Kuril Trench (north-west Pacific Ocean). Deep Sea Res. Part I 74, 39–47.
Klaas, C., Glud, R.N., Wenzhöfer, F., 2023. The expedition PS133/1 of the research vessel Polarstern to the Atlantic Ocean in 2022. In: *Berichte Zur Polar-Und Meeresforschung= Reports on Polar and Marine Research*, p. 774.
Krassowski, M., 2020. ComplexUpset. *ComplexUpset*.
Kurtz, Z.D., Müller, C.L., Miraldi, E.R., Littman, D.R., Blaser, M.J., Bonneau, R.A., 2015. Sparse and compositionally robust inference of microbial ecological networks. PLoS Comput. Biol. 11 (5), e1004226.
Lan, Y., Sun, J., Tian, R., Bartlett, D.H., Li, R., Wong, Y.H., Zhang, W., Qiu, J.W., Xu, T., He, L.S., 2017. Molecular adaptation in the world's deepest-living animal: Insights from transcriptome sequencing of the hadal amphipod Hirondellea gigas. Mol. Ecol. 26 (14), 3732–3743.
Langfelder, P., Horvath, S., 2008. WGCNA: an R package for weighted correlation network analysis. BMC Bioinf. 9, 1–13.
Larkin, M.A., Blackshields, G., Brown, N.P., Chenna, R., McGettigan, P.A., McWilliam, H., Valentin, F., Wallace, I.M., Wilm, A., Lopez, R., 2007. Clustal W and Clustal X version 2.0. *bioinformatics*, *23*(21), 2947-2948.
Lê, S., Josse, J., Husson, F., 2008. FactoMineR: an R package for multivariate analysis. J. Stat. Softw. 25, 1–18.
Leduc, D., Rowden, A.A., 2018. Nematode communities in sediments of the Kermadec trench, Southwest Pacific Ocean. Deep Sea Res. Part I 134, 23–31.
Leduc, D., Rowden, A.A., Glud, R.N., Wenzhöfer, F., Kitazato, H., Clark, M.R., 2016. Comparison between infaunal communities of the deep floor and edge of the Tonga Trench: possible effects of differences in organic matter supply. Deep Sea Res. Part I 116, 264–275.
Leibold, M.A., Holyoak, M., Mouquet, N., Amarasekare, P., Chase, J.M., Hoopes, M.F., Holt, R.D., Shurin, J.B., Law, R., Tilman, D., 2004. The metacommunity concept: a framework for multi-scale community ecology. Ecol. Lett. 7 (7), 601–613.
Leigh, J.W., Bryant, D., Nakagawa, S., 2015. POPART: full-feature software for haplotype network construction. Methods in Ecology & Evolution 6 (9).
Lejzerowicz, F., Esling, P., Majewski, W., Szczuciński, W., Decelle, J., Obadia, C., Arbizu, P.M., Pawlowski, J., 2013. Ancient DNA complements microfossil record in deep-sea subsurface sediments. Biol. Lett. 9 (4), 20130283.
Lejzerowicz, F., Gooday, A.J., Barrenechea Angeles, I., Cordier, T., Morard, R., Apothéloz-Perret-Gentil, L., Lins, L., Menot, L., Brandt, A., Levin, L.A., 2021. Eukaryotic biodiversity and spatial patterns in the Clarion-Clipperton Zone and other abyssal regions: Insights from sediment DNA and RNA metabarcoding. Front. Mar. Sci. 8, 671033.
Liu, J., Du, L., Sun, Z., Zhang, H., 2022. Comparison of structure and diversity of benthic communities in the Okinawa Trough and Mariana Trench by environmental DNA metabarcoding. Deep Sea Res. Part I 185, 103806.
Liu, R., Wang, L., Wei, Y., Fang, J., 2018. The hadal biosphere: recent insights and new directions. Deep Sea Res. Part II 155, 11–18.
Macheriotou, L., Derycke, S., Vanreusel, A., 2023. Environmental filtering along a bathymetric gradient: a metabarcoding meta-analysis of free-living nematodes. Mol. Ecol. 32 (23), 6177–6189.
Macheriotou, L., Guilini, K., Bezerra, T.N., Tytgat, B., Nguyen, D.T., Phuong Nguyen, T. X., Noppe, F., Armenteros, M., Boufahja, F., Rigaux, A., 2019. Metabarcoding free-living marine nematodes using curated 18S and CO1 reference sequence databases for species-level taxonomic assignments. Ecol. Evol. 9 (3), 1211–1226.
Macheriotou, L., Rigaux, A., Derycke, S., Vanreusel, A., 2020. Phylogenetic clustering and rarity imply risk of local species extinction in prospective deep-sea mining areas of the Clarion–Clipperton Fracture Zone. Proc. R. Soc. B 287 (1924), 20192666.
Maroni, P.J., Niyazi, Y., Jamieson, A., 2025. The supergiant amphipod Alicella gigantea may inhabit over half of the world's oceans. R. Soc. Open Sci. 12 (5), 241635.
Martin, M., 2011. Cutadapt removes adapter sequences from high-throughput sequencing reads. Embnet. Journal 17 (1), 10–12.
McMurdie, P.J., Holmes, S., 2013. phyloseq: an R package for reproducible interactive analysis and graphics of microbiome census data. PLoS One 8 (4), e61217.
McPeek, M.A., 1996. Linking local species interactions to rates of speciation in communities. Ecology 77 (5), 1355–1366.
Mehta, R.S., Feder, A.F., Boca, S.M., Rosenberg, N.A., 2019. The relationship between haplotype-based F ST and haplotype length. Genetics 213 (1), 281–295.
Miljutin, D.M., Gad, G., Miljutina, M.M., Mokievsky, V.O., Fonseca-Genevois, V., Esteves, A.M., 2010. The state of knowledge on deep-sea nematode taxonomy: how many valid species are known down there? Mar. Biodivers. 40, 143–159.
Moens, T., Vincx, M., 2000. Temperature, salinity and food thresholds in two brackish-water bacterivorous nematode species: assessing niches from food absorption and respiration experiments. J. Exp. Mar. Biol. Ecol. 243 (1), 137–154.
Moore, J.W., 1979. Influence of food availability and other factors on the composition, structure and density on a subarctic population of benthic invertebrates. Hydrobiologia 62 (3), 215–223.
Pereira, T.J., De Santiago, A., Schuelke, T., Hardy, S.M., Bik, H.M., 2020. The impact of intragenomic rRNA variation on metabarcoding-derived diversity estimates: a case study from marine nematodes. Environ. DNA 2 (4), 519–534.
Ptatscheck, C., Traunspurger, W., 2020. The ability to get everywhere: dispersal modes of free-living, aquatic nematodes. Hydrobiologia 847 (17), 3519–3547.
Rex, M.A., Etter, R.J., Morris, J.S., Crouse, J., McClain, C.R., Johnson, N.A., Stuart, C.T., Deming, J.W., Thies, R., Avery, R., 2006. Global bathymetric patterns of standing stock and body size in the deep-sea benthos. Mar. Ecol. Prog. Ser. 317, 1–8.
Ritchie, H., Jamieson, A., Piertney, S., 2017. Population genetic structure of two congeneric deep-sea amphipod species from geographically isolated hadal trenches in the Pacific Ocean. Deep Sea Res. Part I 119, 50–57.
Rivera Rosas, D.E., Geraldi, N.R., Glud, R.N., Oguri, K., Haond, S.A., Duarte, C.M., 2024. A sedimentary DNA record of the Atacama Trench reveals biodiversity changes in the most productive marine ecosystem. Glob. Chang. Biol. 30 (7), e17412.
Rosli, N., Leduc, D., Rowden, A.A., Probert, P.K., 2018. Review of recent trends in ecological studies of deep-sea meiofauna, with focus on patterns and processes at small to regional spatial scales. Mar. Biodivers. 48, 13–34.
Schauberger, C., Glud, R.N., Hausmann, B., Trouche, B., Maignien, L., Poulain, J., Wincker, P., Arnaud-Haond, S., Wenzhöfer, F., Thamdrup, B., 2021. Microbial community structure in hadal sediments: high similarity along trench axes and strong changes along redox gradients. ISME J. 15 (12), 3455–3467.
Schenk, J., Kleinbölting, N., Traunspurger, W., 2020. Comparison of morphological, DNA barcoding, and metabarcoding characterizations of freshwater nematode communities. Ecol. Evol. 10 (6), 2885–2899.

Schmidt, C., Wolf, K.E., Lins, L., Arbizu, P.M., Brandt, A., 2018. Meiofauna abundance and community patterns along a transatlantic transect in the Vema Fracture Zone and in the hadal zone of the Puerto Rico trench. Deep Sea Res. Part II 148, 223–235.
Schratzberger, M., Ingels, J., 2018. Meiofauna matters: the roles of meiofauna in benthic ecosystems. J. Exp. Mar. Biol. Ecol. 502, 12–25.
Shimabukuro, M., Zeppilli, D., Leduc, D., Wenzhöfer, F., Berg, P., Rowden, A.A., Glud, R. N., 2022. Intra-and inter-spatial variability of meiofauna in hadal trenches is linked to microbial activity and food availability. Sci. Rep. 12 (1), 4338.
Sibly, R., Calow, P., 1983. An integrated approach to life-cycle evolution using selective landscapes. J. Theor. Biol. 102 (4), 527–547.
Sindlev, M., Balmonte, J., Wenzhöfer, F., Xiao, W., Stief, P., Oguri, K., Tsuchiya, M., okoyama, Y., Miyairi, Y., Aze, T., Rudra, A., Canfield, D., Sanei, H., Brandt, A., Glud, R., 2025. The benthic environment of the Aleutian Trench region: Sediment provenance, organic carbon sources and deposition dynamics. *Progress in Oceanography*.
Smith, C.R., De Leo, F.C., Bernardino, A.F., Sweetman, A.K., Arbizu, P.M., 2008. Abyssal food limitation, ecosystem structure and climate change. Trends Ecol. Evol. 23 (9), 518–528.
Somerfield, P.J., 2008. Identification of the Bray-Curtis similarity index: comment on Yoshioka (2008). Mar. Ecol. Prog. Ser. 372, 303–306.
Tang, C.Q., Leasi, F., Obertegger, U., Kieneke, A., Barraclough, T.G., Fontaneto, D., 2012. The widely used small subunit 18S rDNA molecule greatly underestimates true diversity in biodiversity surveys of the meiofauna. Proc. Natl. Acad. Sci. 109 (40), 16208–16212.
Trouche, B., Brandt, M.I., Belser, C., Orejas, C., Pesant, S., Poulain, J., Wincker, P., Auguet, J.-C., Arnaud-Haond, S., Maignien, L., 2021. Diversity and biogeography of bathyal and abyssal seafloor bacteria and archaea along a Mediterranean—Atlantic Gradient. Front. Microbiol. 12, 702016.
Turon, X., Antich, A., Palacín, C., Præbel, K., Wangensteen, O.S., 2020. From metabarcoding to metaphylogeography: separating the wheat from the chaff. Ecol. Appl. 30 (2), e02036.
Vanhove, S., Vermeeren, H., Vanreusel, A., 2004. Meiofauna towards the South Sandwich Trench (750–6300 m), focus on nematodes. Deep Sea Res. Part II 51 (14–16), 1665–1687.
Vanreusel, A., Arbizu, P.M., Yasuhara, M., 2023. Marine Meiofauna Diversity and Biogeography—Paradigms and challenges. In: *New Horizons in Meiobenthos Research: Profiles, Patterns and Potentials*. Springer, pp. 121–151.
Vanreusel, A., Fonseca, G., Danovaro, R., Da Silva, M.C., Esteves, A.M., Ferrero, T., Gad, G., Galtsova, V., Gambi, C., Da Fonsêca Genevois, V., 2010. The contribution of deep-sea macrohabitat heterogeneity to global nematode diversity. Mar. Ecol. 31 (1), 6–20.
Villanueva, R.A.M., Chen, Z.J., 2019. ggplot2: elegant graphics for data analysis. In: Taylor & Francis.
Wei, T., Simko, V., Levy, M., Xie, Y., Jin, Y., Zemla, J., 2017. Package 'corrplot'. Statistician 56 (316), e24.
Weston, J.N.J., Jamieson, A.J., 2022. Exponential growth of hadal science: perspectives and future directions identified using topic modelling. ICES J. Mar. Sci. 79 (4), 1048–1062. https://doi.org/10.1093/icesjms/fsac074.
Zajac, R.N., 2008. Macrobenthic biodiversity and sea floor landscape structure. J. Exp. Mar. Biol. Ecol. 366 (1–2), 198–203.
Zeppilli, D., Leduc, D., Fontanier, C., Fontaneto, D., Fuchs, S., Gooday, A.J., Goineau, A., Ingels, J., Ivanenko, V.N., Kristensen, R.M., 2018. Characteristics of meiofauna in extreme marine ecosystems: a review. Mar. Biodivers. 48, 35–71.
Zeppilli, D., Pusceddu, A., Trincardi, F., Danovaro, R., 2016. Seafloor heterogeneity influences the biodiversity–ecosystem functioning relationships in the deep sea. Sci. Rep. 6 (1), 26352.